J Arid Land (2017) 9(2): 256–269
doi: 10.1007/s40333-017-0007-5

Science Press Springer-Verlag

Drought monitoring and reliability evaluation of the latest TMPA precipitation data in the Weihe River Basin, Northwest China

JIANG Shanhu[1], REN Liliang[1*], ZHOU Meng[1], YONG Bin[1], ZHANG Yu[2], MA Mingwei[3]

[1] State Key Laboratory of Hydrology-Water Resources and Hydraulic Engineering, Hohai University, Nanjing 210098, China;
[2] Department of Civil and Environmental Engineering, Princeton University, Princeton, NJ 08544, USA;
[3] School of Water Conservancy, North China University of Water Resources and Electric Power, Zhengzhou 450045, China

Abstract: The high resolution satellite precipitation products bear great potential for large-scale drought monitoring, especially for those regions with sparsely or even without gauge coverage. This study focuses on utilizing the latest Version-7 TRMM Multi-satellite Precipitation Analysis (TMPA 3B42V7) data for drought condition monitoring in the Weihe River Basin (0.135×10^6 km^2). The accuracy of the monthly TMPA 3B42V7 satellite precipitation data was firstly evaluated against the ground rain gauge observations. The statistical characteristics between a short period data series (1998–2013) and a long period data series (1961–2013) were then compared. The TMPA 3B42V7-based SPI (Standardized Precipitation Index) sequences were finally validated and analyzed at various temporal scales for assessing the drought conditions. The results indicate that the monthly TMPA 3B42V7 precipitation is in a high agreement with the rain gauge observations and can accurately capture the temporal and spatial characteristics of rainfall within the Weihe River Basin. The short period data can present the characteristics of long period record, and it is thus acceptable to use the short period data series to estimate the cumulative probability function in the SPI calculation. The TMPA 3B42V7-based SPI matches well with that based on the rain gauge observations at multiple time scales (i.e., 1-, 3-, 6-, 9-, and 12-month) and can give an acceptable temporal distribution of drought conditions. It suggests that the TMPA 3B42V7 precipitation data can be used for monitoring the occurrence of drought in the Weihe River Basin.

Keywords: TMPA; satellite precipitation; drought monitoring; SPI; Weihe River Basin

Citation: JIANG Shanhu, REN Liliang, ZHOU Meng, YONG Bin, ZHANG Yu, MA Mingwei. 2017. Drought monitoring and reliability evaluation of the latest TMPA precipitation data in Weihe River Basin, Northwest China. Journal of Arid Land, 9(2): 256–269. doi: 10.1007/s40333-017-0007-5

1 Introduction

Drought is a commonly-occurred natural disaster that frequently causes severe economic losses in many countries of the world (Sheffield et al., 2012). China is one of such countries that have constantly suffered from drought disasters (Jun and Chen, 2001). According to the official statistics (Ministry of Water Resources of the People's Republic of China, 2014), the mean annual drought-stricken area in China was up to 0.211×10^6 km^2 and the mean annual grain loss was up to 16.2×10^9 kg during the past ~60 years spanning from 1950 to 2013. Drought is actually an expression of the precipitation deficiency over an extended period of time, leading to a shortage of water supplies (McKee et al., 1993). Thus, timely obtaining accurate precipitation estimates is

*Corresponding author: REN Liliang (E-mail: rll@hhu.edu.cn)
Received 2016-01-14; revised 2016-07-05; accepted 2016-12-03

a prerequisite for a successful drought monitoring (Jiang et al., 2012). However, the traditional ways of assessing drought conditions based on the surface precipitation observations (rain gauge and surface-based weather radar) are often less accurate and normally lack of the needed timeliness and spatial coverage (Jiang et al., 2010, 2014; Mishra and Singh, 2010). During recent years, the growing availability of high-resolution satellite precipitation products provided us with an unprecedented opportunity to monitor drought conditions over a large area and the products are of particular importance for the data scarce or ungauged areas (Kucera et al., 2013; Yong et al., 2014; Zhang et al., 2014; Liu et al., 2016). Nowadays, the satellite precipitation products mainly include the precipitation estimation from remotely sensed information using the artificial neural networks (i.e., PERSIANN), the National Oceanic and Atmospheric Administration Climate Prediction Center morphing technique products (i.e., CMORPH), the tropical rainfall measuring mission (TRMM) multi-satellite precipitation analysis products (i.e., TMPA), and the global precipitation measurement (i.e., GPM) products.

The TMPA precipitation estimates, which combine the low-Earth orbiting microwave data and the geostationary infrared data from all available precipitation-related satellite platforms, were reported to perform the best among many satellite-based precipitation products in the TRMM-era (Huffman et al., 2007). Many studies have demonstrated that the TMPA precipitation data (i.e., TMPA post-real-time research products including TMPA 3B42V6 and TMPA 3B42V7) are acceptable for hydrologic process simulation and also for water resource management (Chen et al., 2013; Xue et al., 2013; Meng et al., 2014; Worqlul et al., 2014; Jiang et al., 2016). The TMPA precipitation data have recently been explored to monitor drought conditions. For example, a comparative analysis between the TMPA and global precipitation climatology centre (GPCC) datasets suggests that it is feasible to use TMPA data for monitoring drought conditions over Africa (Naumann et al., 2012). A work in the Lancang River Basin of southwestern China (Zeng et al., 2012) shows that the TMPA data can be used for drought monitoring in data-scarce regions. TMPA data were shown to be able to monitor drought conditions in the Poyang Lake Basin of southern China (Li et al., 2013a). The TMPA data were also advocated to be adequate for real-time drought monitoring in Indonesia (Vernimmen et al., 2012). And, most recent studies on TMPA-based drought monitoring include Nijssen et al. (2014), Zhou et al. (2014), and Sahoo et al. (2015). These former researches provide us beneficial references for using TMPA satellite precipitation data in drought monitoring. However, at river basin scale, the latest TMPA 3B42V7 data have not been attempted and its acceptability is still unclear. Thus, the present study uses the latest TMPA 3B42V7 data covering the period spanning from 1998 to 2013 to monitor the drought conditions in the Weihe River Basin of northwestern China.

The Weihe River Basin, our study area, has a great strategic significance in the regional economic development and even in the development of the entire West China (Zuo et al., 2014). In recent decades, the Weihe River Basin has experienced several serious droughts with lengthened drought durations and elevated drought severities, resulting in enormous economic losses (Huang et al., 2014). However, the relevant researches were insufficient to support the decision making of the droughts mitigation and the water resource management (Huang et al., 2014). Furthermore, the available meteorological stations within the basin are still insufficient to provide spatially-adequate precipitation data. The high-resolution satellite precipitation data can offer a good alternative in terms of spatial coverage, timeliness and cost efficiency for drought monitoring in the basin.

This study focuses on monitoring drought conditions within the Weihe River Basin during 1998–2013 using the latest TMPA 3B42V7 precipitation data. The accuracy of the TMPA 3B42V7 precipitation data was firstly evaluated using rain-gauge observations. The statistical characteristics between a short-term data (1998–2013) and a long-term data (1961–2013) were then compared to determine the acceptability of using the short-term data series to estimate the cumulative probability function for calculating the drought index. The spatial and temporal patterns of the Standardized Precipitation Index (SPI) were finally depicted based on the TMPA-based monitoring.

2 Study area and data collection

2.1 Study area

The Weihe River is the largest tributary of the Yellow River and the basin covers a drainage area of 0.135×10^6 km^2. The river originates from the Niaoshu Mountains, goes through the provinces of Gansu, Ningxia and Shaanxi, and runs into the Yellow River at the Tongguan Gorge (Fig. 1). The basin extends from 33°50′N to 37°18′N and from 104°00′E to 110°20′E. The elevation within the basin ranges from 304 to 3836 m a.s.l. with a west-east decline. The annual mean temperature ranges between 3.7°C and 13.9°C, and the mean annual precipitation ranges between 400 and 550 mm. The precipitation within the basin is spatially uneven and exhibits a declining trend from southeast to northwest with most of the annual precipitation occurring between July and October. The land uses within the basin include farmlands (46%), pastures (37%), and forests (16%).

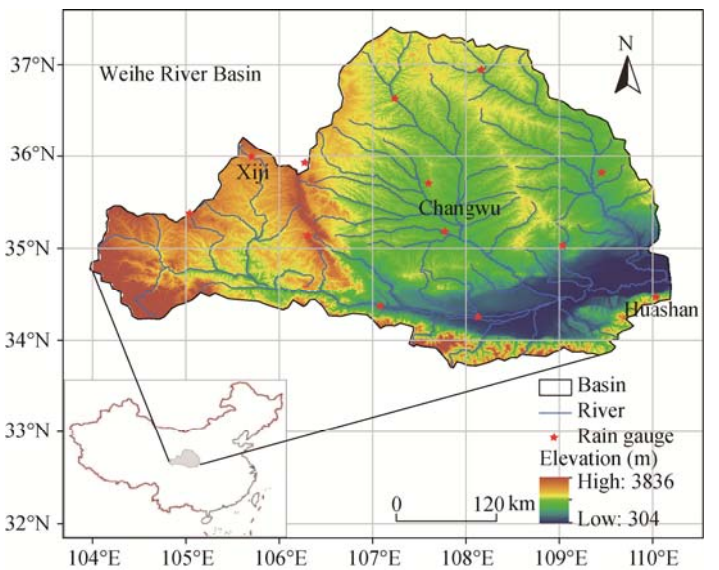

Fig. 1 Location of the Weihe River Basin and the distribution of rain gauge stations. Xiji, Changwu and Huashan are three selected stations representing the upper, middle, and lower reaches of the basin, respectively.

2.2 Data collection

2.2.1 Satellite precipitation data

The TMPA 3B42 post-real-time estimates used in this study were produced in four consecutive steps: (1) the precipitation estimates derived from available Low Earth Orbit (LEO) microwave (MW) radiometers were calibrated using the TRMM combined instrument (TCI) dataset; (2) all of the estimates at 3 h intervals were then merged; (3) the gaps in the analyses were filled using Geosynchronous Earth Orbit (GEO) infrared data that were regionally calibrated to the merged MW product; and (4) a month-to-month bias-adjustment with the global precipitation climatology project (GPCP) data was employed (Huffman et al., 2007). During recent years, the TMPA algorithm has undergone some upgrades to cope with new sensor-resulted data expansion (Yong et al., 2012). The latest upgrade includes the release of the Version-7 of the TMPA satellite precipitation products. It should be mentioned that there are four major upgrades of the TMPA Version-7 over original Version-6. First, the special sensor microwave imager sounder (SSMIS) data on the defence meteorological satellite program (DMSP) F-16 satellites were incorporated into TMPA data to improve the accuracy of microwave precipitation estimates. Second, the TMPA Version-7 used the new global precipitation climatology centre (GPCC) "full" gauge analysis. Third, the non-uniformly processed advanced microwave sounding unit (AMSU) record in Version-6 was uniformly processed in Version-7. Fourth, the TRMM microwave imager (TMI) and the special sensor microwave imager (SSMI) input data were upgraded to the GPROF2010 algorithm (Huffman

and Bolvin, 2013). In this study, we adopted the latest post-real-time research TMPA 3B42V7 satellite precipitation products. The spatial resolution of the TMPA 3B42V7 used in this study is 0.25° and the temporal resolution is 3 h. The 3-h satellite precipitation products were accumulated to form the monthly precipitation products for drought monitoring.

2.2.2 Gauged precipitation data

We collected the precipitation data from 15 meteorological stations for the period of 1961–2013 from the Climatic Data Center, National Meteorological Information Center, China Meteorological Administration, including Xi'an, Tianshui, and Pingliang, which are the stations included in the GPCC gauge analysis. So we only adopted the data from the rest 12 meteorological stations (which are completely independent from those used in the TMPA post-real-time retrieval system) as the benchmark data. These data have been widely used for different studies previously and the quality has been approved to be reliable (Zuo et al., 2014). In addition, three stations (i.e., Xiji, Changwu and Huashan) were selected for graphic presentations of the precipitation in the upper, middle and lower reaches of the basin (Fig. 1), respectively. The inverse distance weighting (IDW) method was first used to interpolate the rain-gauge precipitation onto 0.0625-deg grids and the 0.0625-deg data were then aggregated to 0.25-deg grids to match the spatial resolution of TMPA data (Bartier and Keller, 1996). The topographic data were obtained from the U.S. Geological Survey (USGS) 30 arc-second global digital elevation model (GTOPO30) (https://lta.cr.usgs.gov/GTOPO30).

3 Methodology

3.1 Standardized Precipitation Index (SPI) method

The SPI was first proposed by McKee et al. (1993) to estimate the drought conditions in Colorado. The SPI value for any location can be calculated based on the long-term precipitation record for a designated time period. The proposal was based on an assumption that the precipitation series fit a gamma distribution pattern. The probability density function of precipitation can be expressed as follows:

$$g(x)=\frac{1}{\beta^{\alpha}\Gamma(\alpha)}x^{\alpha-1}e^{-x/\beta},\quad x>0. \tag{1}$$

Where x denotes precipitation value; $\Gamma(\alpha)$ is gamma function; α and β are shape parameter and scale parameter, respectively.

Then, the cumulative probability of precipitation for the given month and time scale for the considered station is computed as:

$$G(x)=\int_0^x g(x)dx=\frac{1}{\beta^{\alpha}\Gamma(\alpha)}\int_0^x x^{\alpha-1}e^{-x/\beta}dx\,. \tag{2}$$

For locations where observations of zero precipitation occur, the fitting of a gamma distribution becomes problematic since it is not defined for zero. In this case, the cumulative probability $H(x)$ becomes:

$$H(x)=q+(1-q)G(x)\,. \tag{3}$$

Where, q is the probability of zero precipitation calculated from the frequency of observations of zero.

When $0<H(x)\le 0.5$,

$$SPI=-\left(t-\frac{\mathrm{c}_0+\mathrm{c}_1t+\mathrm{c}_2t^2}{1+\mathrm{d}_1t+\mathrm{d}_2t^2+\mathrm{d}_3t^3}\right), \tag{4}$$

$$t=\sqrt{\ln\left(\frac{1}{(H(x))^2}\right)}\,. \tag{5}$$

When $0.5<H(x)\le 1$,

$$SPI = t - \frac{c_0 + c_1 t + c_2 t^2}{1 + d_1 t + d_2 t^2 + d_3 t^3}, \tag{6}$$

$$t = \sqrt{\ln\left(\frac{1}{(1 - H(x))^2}\right)}. \tag{7}$$

Where c_0, c_1, c_2, d_1, d_2 and d_3 are calculating parameters, and their values are: c_0=2.515517, c_1=0.802853, c_2=0.010328, d_1=1.432788, d_2=0.189269, and d_3=0.001308; t is the function of $H(x)$.

The fundamental strength of SPI is that it can be calculated for a variety of time scales (i.e., 1-, 3-, 6-, 9- and 12-month). This versatility allows SPI to monitor short-term water supplies, such as seasonal soil moisture availability; and also to monitor long-term water resources, such as groundwater supplies, streamflow amounts, and lake levels (McKee et al., 1993; Mishra and Singh, 2010). Since its initiation, the SPI has been successfully and widely applied in drought monitoring around the world (Hayes et al., 1999; Zhang et al., 2009, Li et al., 2013a). SPI index was divided into 7 classes to indicate either dry conditions or wet conditions (Table 1).

Table 1 Drought and wet classification based on the SPI (Standardized Precipitation Index) index values

SPI	Classes for dryness	SPI	Classes for wetness
0.00– –0.99	Normal (N)	0.00–0.99	Normal (N)
–1.00– –1.49	Moderately dry (MD)	1.00–1.49	Moderately wet (MW)
–1.50– –1.99	Severely dry (SD)	1.50–1.99	Severely wet (SW)
≤–2.00	Extremely dry (ED)	≥2.00	Extremely wet (EW)

3.2 Evaluation statistics

Mean errors (ME), relative bias (BIAS), relative absolute bias (ABIAS), and correlation coefficient (CC) were employed to compare the monthly TMPA satellite precipitation data with rain gauge observations for evaluating the acceptability of the TMPA data in monitoring drought conditions. The ME means the average difference between the satellite-based precipitation estimates and rain gauge observations. The BIAS describes the systematic bias of the satellite-based precipitation estimates, whereas the ABIAS represents the absolute bias of the satellite-based precipitation estimates. The CC indicates the agreement between the satellite-based precipitation estimates and rain gauge observations. The formulas for ME, BIAS, ABIAS and CC are given by following equations.

$$ME = \frac{1}{n}\sum_{i=1}^{n}(S_i - G_i). \tag{8}$$

$$BIAS = \frac{\sum_{i=1}^{n}(S_i - G_i)}{\sum_{i=1}^{n} G_i} \times 100\%. \tag{9}$$

$$ABIAS = \frac{\sum_{i=1}^{n}|S_i - G_i|}{\sum_{i=1}^{n} G_i} \times 100\%. \tag{10}$$

$$CC = \frac{\sum_{i=1}^{n}(G_i - \overline{G})(S_i - \overline{S})}{\sqrt{\sum_{i=1}^{n}(G_i - \overline{G})^2}\sqrt{\sum_{i=1}^{n}(S_i - \overline{S})^2}}. \tag{11}$$

Where n is the total sets of rain gauge data or satellite precipitation data; S_i and G_i are the i^{th}

values of the satellite-based precipitation data and rain gauge observations, respectively; and $\overline{S}$ and $\overline{G}$ are the mean values of the satellite-based precipitation data and rain gauge observations, respectively.

In addition, the validation statistical indices of CC and the categorical statistical indices of critical success index (CSI) were adopted to measure the correspondence between the satellite-based drought estimates and rain gauge-based drought estimates. The CC shows the agreement between the satellite-based SPI and rain gauge-based SPI. The CSI represents the proportion of the times of drought events (as well as flood events) that were correctly diagnosed by the TMPA satellite-based precipitation data (Zeng et al., 2012). The drought events (as well as flood events) are defined in the Table 1. The perfect value of CSI is 1.0. The formula of CSI is given by the following equation:

$$CSI = \frac{t_{\mathrm{H}}}{t_{\mathrm{H}} + t_{\mathrm{M}} + t_{\mathrm{F}}}. \tag{12}$$

Where H, M, and F are different cases; H, observed drought events that were also correctly diagnosed by satellite-based precipitation data; M, observed drought events that were not diagnosed; F, drought events that were diagnosed but not observed; and t_{H}, t_{M} and t_{F} are the times of occurrence of the corresponding case (see details in Ebert et al. (2007)).

4 Results and discussion

4.1 Comparison of TMPA data with rain gauge observations

The statistical indices (i.e. ME, BIAS, ABIAS and CC) were first calculated to compare the TMPA 3B42V7 precipitation data with rain gauge observations at both station and basin scales. Table 2 includes the statistical indices of TMPA 3B42V7 and rain gauge precipitation data at monthly time scale. Table 2 shows that the ME ranges from –4.39 to 4.95 mm; the BIAS ranges from –7.09% to 11.72%; the ABIAS ranges from 20.09% to 32.96%; and the CC ranges from 0.90 to 0.95. It can be seen that the differences between TMPA 3B42V7 data and rain gauge observations are generally small and TMPA 3B42V7 data are thus acceptable for drought monitoring. But, the ABIAS is still too large and the distribution of the TMPA 3B42V7 at monthly or sub-monthly time scale thus still needs to be improved. Generally speaking, the TMPA 3B42V7 slightly overestimated the precipitation with exceptions at following four stations: Baoji, Wugong, Luochuan, and Huashan. Figure 2 is the scatter plots of three representative stations (i.e., Xiji, Changwu and Huashan) and the basin average at monthly time scale. It can be seen that linear relationships between the TMPA data and rain gauge observations are rather robust and the CC is 0.91 (R^2=0.82) at Xiji, 0.92 (R^2=0.85) at Changwu, and 0.95 (R^2=0.91) at Huashan. It is quite notable that CC is as high as 0.98 (R^2=0.97) at basin scale (i.e., basin average), demonstrating that the TMPA 3B42V7 precipitation data are acceptable for monitoring drought conditions in the Weihe River basin.

Table 2 Comparison of statistical indices between TMPA 3B42V7 estimates and rain gauge observations at monthly time scale

Station	ME (mm)	BIAS (%)	ABIAS (%)	CC	Station	ME (mm)	BIAS (%)	ABIAS (%)	CC
Huajialing	1.06	2.73	22.20	0.95	Wugong	–1.41	–2.81	27.95	0.90
Xiji	3.72	11.72	32.96	0.91	Wuqi	3.30	8.51	27.64	0.94
Guyuan	3.77	10.52	31.65	0.91	Tongchuan	0.58	1.13	26.65	0.91
Baoji	–1.24	–2.29	25.70	0.91	Luochuan	–0.41	–0.79	26.26	0.93
Huanxian	4.11	11.67	29.99	0.93	Huashan	–4.39	–7.09	20.09	0.95
Xifengzhen	4.95	10.88	24.37	0.95	Basin average	2.40	5.40	11.44	0.98
Changwu	4.70	9.64	26.53	0.92					

Note: ME, mean errors; BIAS, relative bias; ABIAS, relative absolute bias; CC, correlation coefficient.

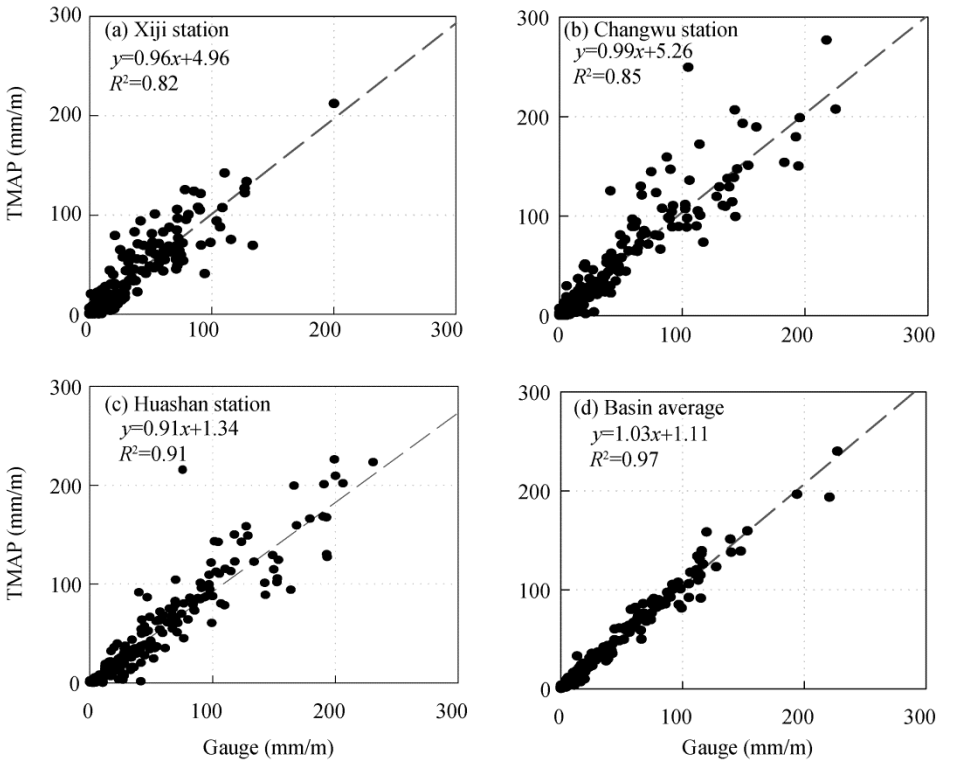

Fig. 2 Precipitation scatter plots of three representative stations (a–c) and the basin average (d). TMPA, TMPA 3B42V7 precipitation estimates at monthly time scale. Gauge represents rain gauge observations at monthly time scale.

Figure 3a shows the spatially-distributed patterns of the rain-gauged mean annual precipitation and Figure 3b shows the spatial distribution of TMPA-estimated precipitation. The spatial similarity between these two patterns (Figs. 3a and b) is rather high with more details expressed in Figure 3b (i.e., TMPA-estimated precipitation). We speculate that Figure 3b is a more realistic spatial expression of the annual precipitation than Figure 3a. Our speculation is based on following three facts. First, Figure 3a was interpolated based on a limited number of rain gauge observations. Second, Figure 3b was estimated based on sufficient data points (TMPA 3B42V7 cells). Third, the average CC between TMPA 3B42V7 data and rain gauge observations at those 12 participating stations was as high as 0.98.

4.2 Statistical comparison between short-term and long-term series

The TMPA 3B42V7 data became available only from January 1998 onward and its limited time length is a major restriction for fitting a long-term probability distribution function (Naumann et al., 2012; Li et al., 2013b). Thus, we investigated the robustness of the short-term data (1998–2013) for fitting a long-term probability distribution function. We firstly analyzed the coincidence of several statistical indices, such as monthly mean (Mean), maximal (Max), minimal (Min) and standard deviation (Std), between a long-term (1961–2013) and a short-term (1998–2013) rain-gauge observations at three representative rain-gauge stations (Xiji, Changwu and Huashan) and also at basin scale (i.e., basin average). Table 3 shows that the long-term Mean was 34.05 mm at Xiji, 48.62 mm at Changwu, 67.60 mm at Huashan, and 45.16 mm at basin scale. The short-term Mean was 31.73 mm at Xiji, 48.77 mm at Changwu, 61.93 mm at Huashan, and 44.38 mm at basin scale. It means that the short-term monthly means are all not significantly different from the long-term monthly means. It should be stressed that other statistical indices (e.g., Max, Min and Std) are also similar between the long-term (1961–2013) and the short-term (1998–2013) data series. Table 3 also shows that the short-term (1998–2013) rain-gauged monthly means at the three representative stations and also at the basin scale (i.e., basin average) are all not

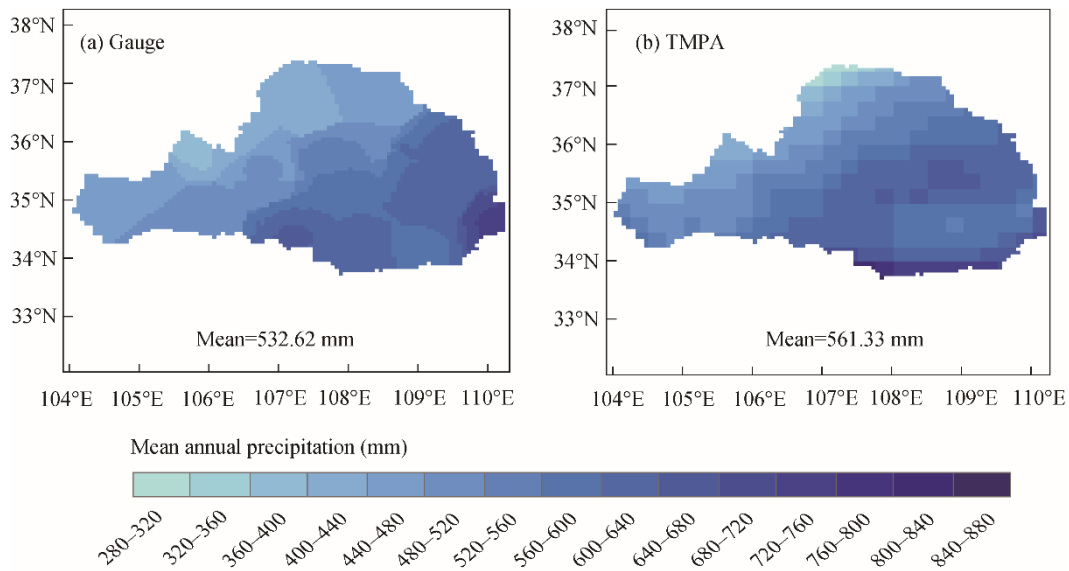

Fig. 3 Spatial distributions of mean annual precipitation based on rain gauge observations (a) and TMPA 3B42V7 estimates from 1998 to 2013 (b)

significantly different from the short-term TMPA-inferred monthly means. And, other statistical indices (e.g., Max, Min, and Std) are also quite similar between the rain-gauged monthly means and the TMPA-inferred monthly means for the data overlapping period (1998–2013). Figure 4 is the comparisons of monthly mean precipitation data series between the short-term (1998–2013) and the long-term (1961–2013) and also between rain-gauge observations and TMPA 3B42V7 estimates. Figure 4 shows that the short-term TMPA 3B42V7 estimates are generally similar to both the short-term and the long-term rain-gauge observations at the three representative stations. In comparison, the TMPA 3B42V7 estimates are almost identical with both the short-term and the long-term rain-gauge observations. Our results are quite consistent with those of Li et al. (2013b). The aforementioned similarities suggest that a short-term data series can be used for fitting a long-term probability distribution function.

4.3 TMPA-inferred temporal variation of drought conditions

The SPI values at different time scales were computed for each grid (0.25°×0.25°) in the Weihe River Basin using the monthly TMPA precipitation data from January 1998 to December 2013.

Table 3 Comparison of statistical indices between short-term (1998–2013) and long-term (1961–2013) data series

Station	Data set	Mean (mm/m)	Max (mm/m)	Min (mm/m)	Std (mm/m)
Xiji	Gauge 1961–2013	34.05	226.40	0.00	39.15
	Gauge 1998–2013	31.73	200.20	0.00	35.24
	TMPA 1998–2013	35.45	212.17	0.00	37.31
Changwu	Gauge 1961–2013	48.62	312.00	0.00	51.37
	Gauge 1998–2013	48.77	312.00	0.00	53.32
	TMPA 1998–2013	53.47	276.87	0.00	57.25
Huashan	Gauge 1961–2013	67.60	328.70	0.00	61.92
	Gauge 1998–2013	61.93	328.70	0.00	61.11
	TMPA 1998–2013	57.54	309.20	0.00	58.28
Basin average	Gauge 1961–2013	45.16	227.17	0.00	43.89
	Gauge 1998–2013	44.38	227.17	0.09	44.48
	TMPA 1998–2013	46.78	240.03	0.16	46.48

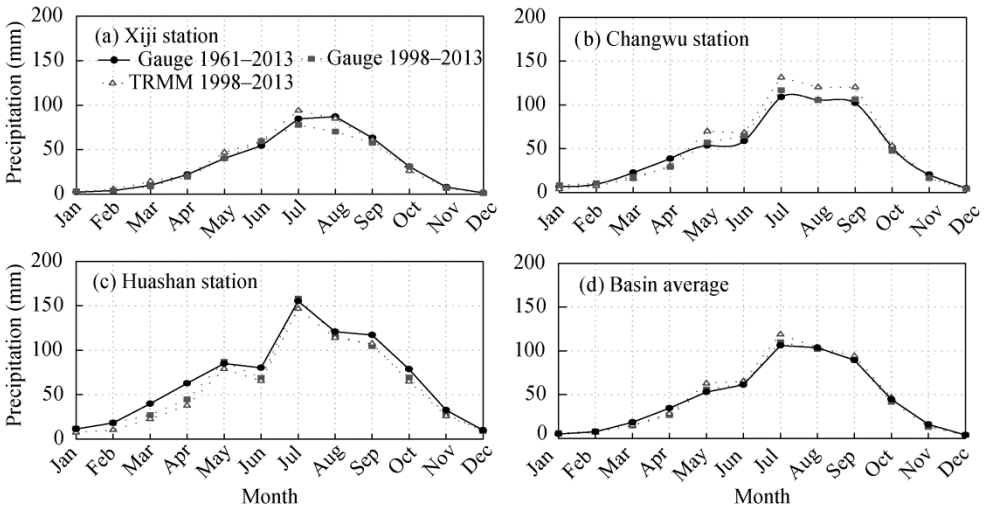

Fig. 4 Comparisons of monthly mean precipitation between the short-term (1998–2013) and the long-term (1961–2013) data series and also between rain gauge observations and TMPA 3B42V7 estimates

And, the rain gauge observations were also used to calculate the SPI. A positive SPI means that the precipitation over a designated period was higher than that over the whole time series, while a negative SPI indicates that the precipitation over a designated period was lower than that over the whole time series.

At 1-month scale, the CC between TMPA-based SPI and rain gauge-based SPI is 0.64 (R^2=0.41) in Xiji, 0.78 (R^2=0.61) at Changwu, 0.86 (R^2=0.74) at Huashan and 0.92 (R^2=0.86) at basin scale (Table 4; Fig. 5). Generally speaking, the TMPA-based SPI has good consistency with the rain gauge based-SPI. Figure 6 shows the occurrence frequency (%) of the different dry and wet classes expressed both by TMPA-inferred SPI_1 and by rain-gauged SPI_1. The normal class (i.e., $-0.99 \leq SPI_1 \leq 0.99$) had the largest share, accounting for 60%–70%, and the extremely dry class (ED) and extremely wet class (EW) had the lowest frequency, being less than 5%. The other classes including moderately dry (MD), moderately wet (MW), severely dry (SD) and severely wet (SW) varied between 3% and 15%. Again, the high degree of temporal coincidence between the TMPA-inferred SPI_1 and the rain-gauged SPI_1 means that the TMPA 3B42V7 data can be used to determine the dry and wet classes in the Weihe River Basin.

Table 4 Validation of different time scales TMPA-based SPI

Station	SPI_1		SPI_3		SPI_6		SPI_9		SPI_{12}	
	CC	CSI (%)	CC	CSI (%)	CC	CSI (%)	CC	CSI (%)	CC	CSI (%)
Huajialing	0.78	68.23	0.81	66.15	0.85	61.98	0.86	62.50	0.88	61.98
Xiji	0.64	60.94	0.64	60.42	0.70	59.90	0.72	63.54	0.70	59.38
Guyuan	0.70	65.63	0.64	63.54	0.74	66.67	0.74	69.27	0.70	65.10
Baoji	0.75	69.27	0.74	67.71	0.82	73.44	0.85	69.27	0.87	71.35
Huanxian	0.74	66.15	0.80	64.58	0.84	61.46	0.80	55.73	0.78	54.17
Xifengzhen	0.82	68.75	0.81	65.63	0.88	71.35	0.91	78.65	0.93	80.21
Changwu	0.80	61.98	0.76	69.27	0.77	65.10	0.73	66.67	0.75	70.83
Wugong	0.82	76.56	0.82	65.10	0.85	72.92	0.88	69.27	0.90	70.31
Wuqi	0.75	66.15	0.81	71.35	0.89	67.71	0.90	61.98	0.90	58.85
Tongchuan	0.81	68.23	0.81	67.19	0.82	59.90	0.79	61.46	0.81	59.90
Luochuan	0.82	62.50	0.81	67.19	0.81	61.98	0.79	60.42	0.82	59.38
Huashan	0.86	73.44	0.87	67.19	0.87	69.27	0.88	65.63	0.89	65.10
Basin Average	0.92	80.73	0.92	78.13	0.96	85.42	0.96	85.94	0.97	86.46

Note: CC, correlation coefficient; CSI, critical success index.

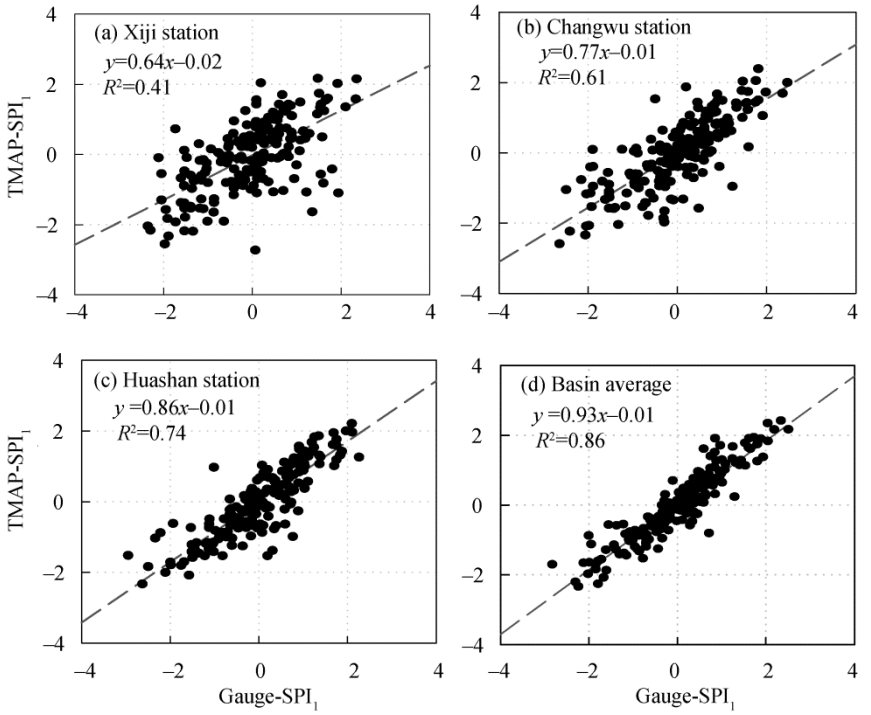

Fig. 5 SPI_1 scatter plots of three representative stations (a–c) and the basin average (d). TMPA-SPI_1, TMPA-inferred SPI_1 estimates; Gauge-SPI_1, rain gauged SPI_1.

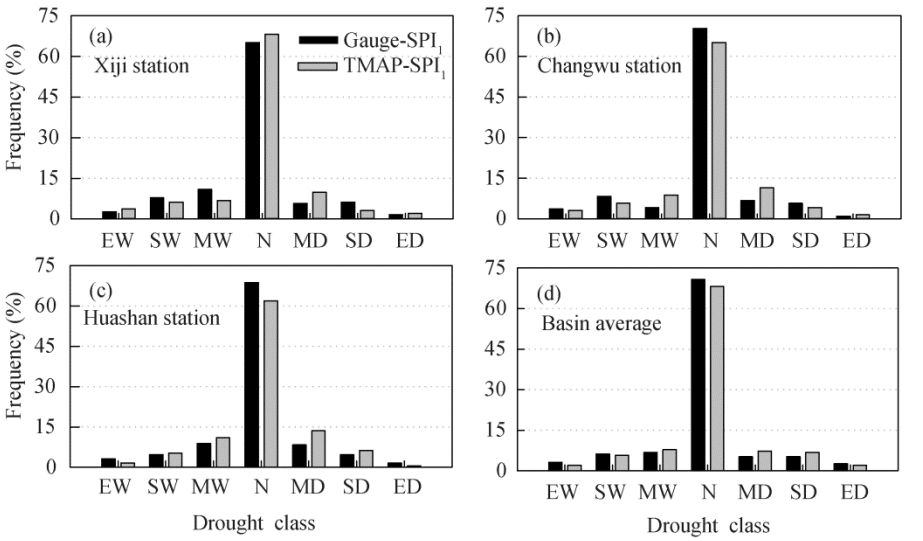

Fig. 6 Occurrence frequencies (%) of the different dry and wet classes based both on rain gauged SPI_1 and TMPA-inferred SPI_1. EW, extremely wet; SW, severely wet; MW, moderately wet; N, normal; MD, moderately dry; SD, severely dry; ED, extremely dry.

For comparing the results in different time scales, we computed the statistical indices at 1-, 3-, 6-, 9- and 12-month scales (Table 4). Table 4 shows that the CC between the rain-gauged SPI_1 and the TMPA-inferred SPI_1 ranged from 0.64 to 0.86 and the CSI ranged from 60.94% to 76.56%, indicating that the TMPA-based SPI estimation is an acceptable tool for drought monitoring in the Weihe River Basin. Furthermore, the results at 3-, 6-, 9- and 12-month scales are similar with the result of 1-month scale, again meaning that the TMPA-based SPI estimation is an acceptable tool for drought monitoring at different time scales in the Weihe River Basin. Figure 7 shows the

inter-annual variability of SPI based on TMPA 3B42V7 estimates and rain gauge observations at different time scales at basin scale (i.e., basin average). It shows that the TMPA 3B42V7-based SPI matches the rain gauge-based SPI very well at all time scales (1-, 3-, 6-, 9- and 12-month scales), again confirming that the TMPA 3B42V7 data have great potentials for the drought monitoring in the Weihe River Basin and probably also in other areas.

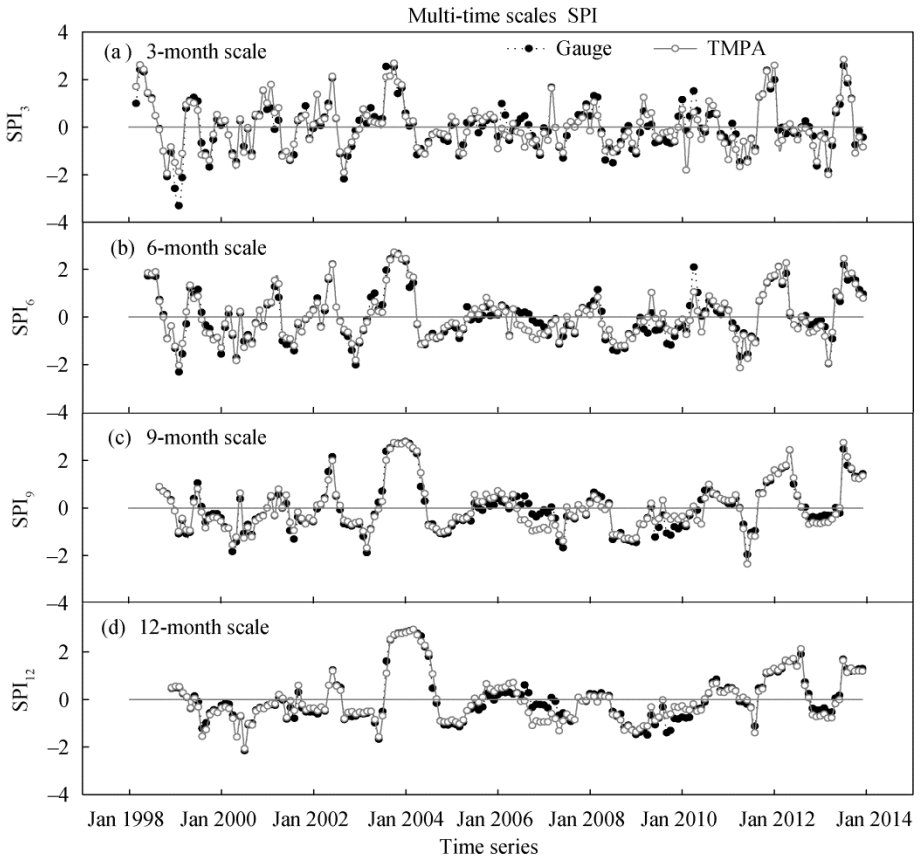

Fig. 7 Comparison of SPI time series calculated both from rain gauge observations and from TMPA 3B42V7 estimates at 3-month scale (a), 6-month scale (b), 9-month scale (c), and 12-month scale (d)

Table 5 Validation of SPI_1 for two typical drought events: one occurred in the period spanning from March to August 2000, and the other occurred in the period spanning from October 2012 to March 2013

Period	Description of the drought event	Gauge-SPI_1	TMPA-SPI_1	Classification	
				Gauge	TMPA
Mar 2000	The drought affected a wide area with not only severe drought but also long drought period.	–0.80	–0.87	Normal	Normal
Apr 2000		–0.35	–0.52	Normal	Normal
May 2000		–1.21	–1.38	Moderately dry	Moderately dry
Jun 2000		1.89	1.90	Severely wet	Severely wet
Jul 2000		–1.66	–2.08	Severely dry	Extremely dry
Aug 2000		0.24	0.49	Normal	Normal
Oct 2012	The precipitation has been 50% below normal value, and this change leads to a severe drought in the next spring.	–1.79	–1.61	Severely dry	Severely dry
Nov 2012		0.02	0.11	Normal	Normal
Dec 2012		0.21	–0.08	Normal	Normal
Jan 2013		–0.70	–0.85	Normal	Normal
Feb 2013		0.39	0.40	Normal	Normal
Mar 2013		–1.60	–1.87	Severely dry	Severely dry

To further evaluate the reliability of using the TMPA 3B42V7 data to monitor drought conditions, we targeted two typical drought events as validation cases: one occurred in the period spanning from March to August 2000 and the other occurred in the period spanning from October 2012 to March 2013. The validation demonstrated that TMPA 3B42V7-inferred SPI captured the drought events very well in both cases (Table 5). In both cases, the TMPA 3B42V7 told almost exactly the same stories as the rain gauge did, again further confirming that the TMPA 3B42V7 data have great potentials for the drought monitoring in the Weihe River Basin and probably also in other areas.

5 Conclusions

This paper evaluated the reliability of drought monitoring using the latest TMPA 3B42V7 in the Weihe River Basin. The results revealed that the monthly TMPA 3B42V7 precipitation is in a high agreement with the rain gauge observations and can accurately capture the temporal and spatial characteristics of rainfall within the Weihe River Basin. The characteristics of TMPA 3B42V7 data over a short period (1998–2013) can present the characteristics of long period (1961–2013) records. Thus, it is acceptable for using the short period data series to estimate the cumulative probability function in the SPI drought index calculation. The variabilities of TMPA 3B42V7-based SPI and rain gauge observations-based SPI were similar at multiple time scales (1-, 3-, 6-, 9- and 12-month) and can give an acceptable temporal distribution of drought conditions. Generally speaking, TMPA 3B42V7 precipitation data can be used for monitoring the occurrence of drought disasters in the Weihe River Basin.

Finally, we want to make a note that the GPM mission, as an extended satellite precipitation observation plan of TMPA mission, provides the users more accurate and higher spatial-resolution and higher temporal-resolution precipitation products named Integrated Multi-satellite Retrievals for GPM (IMERG; 0.1–0.5 h) (Hou et al., 2014). The GPM products are making improvements in areas such as spatial and temporal resolutions and snowfall estimates, etc. (Liu, 2016; Tang et al., 2016). It is widely believed that combining the ongoing GPM data with the existing TMPA data can provide a golden opportunity in the near future for large-scale and timely drought monitoring (Kucera et al., 2013; Tao et al., 2016).

Acknowledgments

This study was jointly supported by the National Key Research and Development Program approved by Ministry of Science and Technology, China (2016YFA0601504), the Program of Introducing Talents of Discipline to Universities by the Ministry of Education and the State Administration of Foreign Experts Affairs, China (B08048), the National Natural Science Foundation of China (41501017, 51579066) and the Natural Science Foundation of Jiangsu Province (BK20150815).

References

Bartier P M, Keller C P. 1996. Multivariate interpolation to incorporate thematic surface data using inverse distance weighting (IDW). Computers & Geosciences, 22(7): 795–799.

Chen Y J, Ebert E E, Walsh K J E, et al. 2013. Evaluation of TRMM 3B42 precipitation estimates of tropical cyclone rainfall using PACRAIN data. Journal of Geophysical Research: Atmospheres, 118(5): 2184–2196.

Ebert E E, Janowiak J E, Kidd C. 2007. Comparison of near-real-time precipitation estimates from satellite observations and numerical models. Bulletin of the American Meteorological Society, 88(1): 47–64.

Hayes M J, Svoboda M D, Wilhite D A, et al. 1999. Monitoring the 1996 drought using the standardized precipitation index. Bulletin of the American Meteorological Society, 80(3): 429–438.

Hou A Y, Kakar R K, Neeck S, et al. 2014. The global precipitation measurement mission. Bulletin of the American Meteorological Society, 95(5): 701–722.

Huang S Z, Chang J X, Huang Q, et al. 2014. Spatio-temporal changes and frequency analysis of drought in the Wei River basin, China. Water Resources Management, 28(10): 3095–3110.

Huffman G J, Bolvin D T, Nelkin E J, et al. 2007. The TRMM Multisatellite Precipitation Analysis (TMPA): quasi-global, multiyear, combined-sensor precipitation estimates at fine scales. Journal of Hydrometeorology, 8(1): 38–55.

Huffman G J, Bolvin D T. 2013. Real-time TRMM multi-satellite precipitation analysis data set documentation. [2015-06-17]. ftp://meso-a.gsfc.nasa.gov/pub/trmmdocs/rt/3B4XRT_doc_V7.pdf.

Jiang S H, Ren L L, Yong B, et al. 2010. Evaluation of high-resolution satellite precipitation products with surface rain gauge observations from Laohahe Basin in northern China. Water Science and Engineering, 3(4): 405–417.

Jiang S H, Ren L L, Hong Y, et al. 2012. Comprehensive evaluation of multi-satellite precipitation products with a dense rain gauge network and optimally merging their simulated hydrological flows using the Bayesian model averaging method. Journal of Hydrology, 452–453: 213–225.

Jiang S H, Ren L L, Hong Y, et al. 2014. Improvement of multi-satellite real-time precipitation products for ensemble streamflow simulation in a middle latitude basin in South China. Water Resources Management, 28(8): 2259–2278.

Jiang S H, Ren L L, Yong B, et al. 2016. Evaluation of latest TMPA and CMORPH precipitation products with independent rain gauge observation networks over high-latitude and low-latitude basins in China. Chinese Geographical Science, 26(4): 439–455.

Jun X, Chen Y Q. 2001. Water problems and opportunities in the hydrological sciences in China. Hydrological Sciences Journal, 46(6): 907–921.

Kucera P A, Ebert E E, Turk F J, et al. 2013. Precipitation from space: advancing earth system science. Bulletin of the American Meteorological Society, 94(3): 365–375.

Li X H, Zhang Q, Ye X C. 2013a. Dry/wet conditions monitoring based on TRMM rainfall data and its reliability validation over Poyang Lake Basin, China. Water, 5(4): 1848–1864.

Li X H, Zhang Q, Ye X C. 2013b. Capabilities of satellite-based precipitation to estimate the spatiotemporal variation of flood/drought class in Poyang Lake Basin. Advances in Meteorology, 2013: 901240.

Liu X F, Zhu X F, Pan Y Z, et al. 2016. Agricultural drought monitoring: Progress, challenges, and prospects. Journal of Geographical Sciences, 26(6): 750–767.

Liu Z. 2016. Comparison of integrated multisatellite retrievals for GPM (IMERG) and TRMM multisatellite precipitation analysis (TMPA) monthly precipitation products: initial results. Journal of Hydrometeorology, 17(3): 777–790.

McKee T B, Doesken N J, Kleist J. 1993. The relationship of drought frequency and duration to time scales. In: Paper Presented at 8th Conference on Applied Climatology. Anaheim, CA, American Meteorology Society, 174–184.

Meng J, Li L, Hao Z C, et al. 2014. Suitability of TRMM satellite rainfall in driving a distributed hydrological model in the source region of Yellow River. Journal of Hydrology, 509: 320–332.

Ministry of Water Resources of the People's Republic of China. 2014. Bulletin of Flood and Drought Disasters in China, 2013. Beijing: China Water Power Press, 37–38. (in Chinese)

Mishra A K, Singh V P. 2010. A review of drought concepts. Journal of Hydrology, 391(1–2): 202–216.

Naumann G, Barbosa P, Carrao H, et al. 2012. Monitoring drought conditions and their uncertainties in Africa using TRMM data. Journal of Applied Meteorology and Climatology, 51(10): 1867–1874.

Nijssen B, Shukla S, Lin C Y, et al. 2014. A prototype global drought information system based on multiple land surface models. Journal of Hydrometeorology, 15(4): 1661–1676.

Sahoo A K, Sheffield J, Pan M, et al. 2015. Evaluation of the tropical rainfall measuring mission multi-satellite precipitation analysis (TMPA) for assessment of large-scale meteorological drought. Remote Sensing of Environment, 159: 181–193.

Sheffield J, Wood E F, Roderick M L. 2012. Little change in global drought over the past 60 years. Nature, 491(7424): 435–438.

Tang G Q, Zeng Z Y, Long D, et al. 2016. Statistical and hydrological comparisons between TRMM and GPM level-3 products over a midlatitude basin: is day-1 IMERG a good successor for TMPA 3B42V7?. Journal of Hydrometeorology, 17(1): 121–137.

Tao H, Fischer T, Zeng Y, et al. 2016. Evaluation of TRMM 3B43 precipitation data for drought monitoring in Jiangsu Province, China. Water, 8(6): 221.

Vernimmen R R E, Hooijer A, Mamenun, et al. 2012. Evaluation and bias correction of satellite rainfall data for drought monitoring in Indonesia. Hydrology and Earth System Sciences, 16(1): 133–146.

Worqlul A W, Maathuis B, Adem A A, et al. 2014. Comparison of rainfall estimations by TRMM 3B42, MPEG and CFSR with ground-observed data for the Lake Tana basin in Ethiopia. Hydrology and Earth System Sciences, 18(12): 4871–4881.

Xue X W, Hong Y, Limaye A S, et al. 2013. Statistical and hydrological evaluation of TRMM-based multi-satellite precipitation analysis over the Wangchu basin of Bhutan: are the latest satellite precipitation products 3B42V7 ready for use in ungauged basins?. Journal of Hydrology, 499: 91–99.

Yong B, Hong Y, Ren L L, et al. 2012. Assessment of evolving TRMM-based multisatellite real-time precipitation estimation methods and their impacts on hydrologic prediction in a high latitude basin. Journal of Geophysical Research: Atmospheres, 117(D9): D09108.

Yong B, Chen B, Gourley J J, et al. 2014. Intercomparison of the Version-6 and Version-7 TMPA precipitation products over high and low latitudes basins with independent gauge networks: is the newer version better in both real-time and post-real-time analysis for water resources and hydrologic extremes?. Journal of Hydrology, 508: 77–87.

Zeng H W, Li L J, Li J Y. 2012. The evaluation of TRMM Multisatellite Precipitation Analysis (TMPA) in drought monitoring in the Lancang river basin. Journal of Geographical Sciences, 22(2): 273–282.

Zhang Q, Xu C Y, Zhang Z X. 2009. Observed changes of drought/wetness episodes in the Pearl River basin, China, using the standardized precipitation index and aridity index. Theoretical and Applied Climatology, 98(1–2): 89–99.

Zhang Y, Hong Y, Wang X G, et al. 2014. Hydrometeorological analysis and remote sensing of extremes: was the July 2012 Beijing flood event detectable and predictable. Journal of Hydrometeorology, 16(1): 381–395.

Zhou T, Nijssen B, Huffman G J, et al. 2014. Evaluation of real-time satellite precipitation data for global drought monitoring. Journal of Hydrometeorology, 15(4): 1651–1660.

Zuo D P, Xu Z X, Wu W, et al. 2014. Identification of streamflow response to climate change and human activities in the Wei River Basin, China. Water Resources Management, 28(3): 833–851.